(Received 9 September 2025, Accepted 11 November 2025, Scheduled 16 November 2025)

Wavelet-Based Time-Frequency Analysis of Ultrashort Laser Pulses

Mounir Khelladi[1,*] and Djelloul Aissaoui[2]

[1] *Telecommunication Department, Faculty of Technology, University of Tlemcen, Tlemcen 13000, Algeria*
[2] *Telecommunications and Smart Systems Laboratory, Ziane Achour University of Djelfa, PO Box 3117, Djelfa 17000, Algeria*

ABSTRACT: An original computational framework is developed to simulate the propagation of ultrashort laser pulses with arbitrary temporal and spectral profiles through uniform linear dielectric materials. The study investigates how spectral phase sampling during propagation affects computational efficiency and accuracy. The proposed approach enables a comprehensive analysis of ultrashort pulse evolution in both the time and frequency domains. To demonstrate its effectiveness, the algorithm is applied to various propagation phenomena, such as temporal and spectral shifts, pulse broadening, asymmetric distortions, and chirping in dispersive media, using a wavelet-based time-frequency decomposition.

1. INTRODUCTION

The propagation of ultrashort optical pulses through linear media has been extensively investigated using analytical approaches applied to systems such as free space [1–5], dispersive materials [6, 7], diffractive optics [8, 9], focusing components [10–12], and apertures [13–16].

However, only a limited number of numerical simulations have been reported. Most existing studies rely on analytical formulations based on simplified pulse models, typically assuming plane-wave or TEM_{00} Gaussian spatial distributions combined with Gaussian temporal profiles. For example, Sheppard and Gan [3] analyzed spectral transformations in Gaussian pulsed beams, while Agrawal [4] examined spatial broadening effects in diffracted pulses with Gaussian spatial and temporal shapes.

Although these analytical approaches provide useful insight, they cannot easily accommodate arbitrary pulse shapes, and closed-form solutions often require significant approximations. To overcome these limitations, numerical simulation methods have emerged as powerful alternatives for studying pulse propagation dynamics. A major step was achieved by Kaplan [5], who introduced a fast Fourier transform (FFT)-based model allowing detailed temporal analysis of arbitrarily profiled pulses.

Recent breakthroughs in ultrashort pulse propagation research have highlighted critical limitations in classical analytical techniques and underscored the need for a robust numerical framework capable of modeling the full complexity of pulse evolution. In addition, recent studies have demonstrated the relevance of advanced wavelet-based signal processing tools to characterize broadband ultrashort pulses with improved time-frequency localization, enabling a deeper understanding of spectral distortions, chirp evolution, and phase-induced shaping mechanisms during propagation [24–27]. These developments further confirm the need for efficient computational techniques capable of capturing both temporal and spectral dynamics in dispersive media.

* Corresponding author: Mounir Khelladi (mo.khelladi@gmail.com).

In this context, we present a comprehensive computational approach for simulating ultrashort pulse propagation in linear, homogeneous media. Building upon wave-optical field representation theory [17], our method offers three major advantages: (1) simplified computation of pulsed field merit functions, (2) joint time-frequency domain analysis at arbitrary propagation planes, and (3) efficient tracking of spectral and temporal evolution over any distance. The proposed framework models propagation through its spectral equivalent, introducing optimized phase-sampling rules that ensure numerical accuracy while reducing the number of required spectral components. These criteria significantly enhance computational efficiency, making the method suitable for broadband ultrashort pulse analysis.

2. FEMTOSECOND-SCALE TEMPORAL RESOLUTION

This relationship becomes particularly significant for few-cycle pulses, where the Fourier transform limitation defines the shortest achievable duration for a given spectral width. Mathematically, this can be expressed as $\tau \cdot \Delta w \geq K$, where K is a numerical constant depending on the pulse shape and the definitions used for duration and bandwidth.

$$\tau \cdot \Delta w \geq 2 \cdot \pi \cdot c_B$$

The parameter c_B represents a pulse-shape-dependent constant, while w denotes the angular frequency. This relationship is fundamentally connected to both temporal frequency (f) and wavelength (λ) through the following expressions:

$$w = 2 \cdot \pi \cdot f = \frac{2 \cdot \pi \cdot c}{\lambda} \tag{1}$$

Equation (1) reveals two fundamental principles of ultrashort pulse generation: First, the pulse duration is fundamentally limited by the available spectral bandwidth, requiring extremely broad spectra for shorter pulses. Second, the transform-limited

condition represents the theoretical minimum duration achievable for a given spectrum, where all frequency components remain perfectly phase-aligned in time.

The time-bandwidth relationship in Equation (1) establishes an inequality ($\tau \cdot \Delta w \geq 2\pi cB$), where equality indicates a transform-limited pulse, and higher values correspond to chirped pulses with temporally dispersed frequency components.

This chirping phenomenon arises when the spectral phase becomes nonuniform, introducing a frequency modulation across the pulse envelope. In practice, ultrashort pulse systems often operate beyond the transform limit due to intentional chirping for amplification **or** unavoidable dispersion effects during propagation.

2.1. Theoretical Framework for Ultrashort Pulse Characterization

Ultrashort laser pulses are coherent electromagnetic wave packets characterized by their temporal coherence, spatial coherence (beam quality and focusing properties), temporal contrast, and peak power. While these pulses exhibit complex spatiotemporal characteristics, this work focuses specifically on their temporal-domain behavior.

2.1.1. Time-Resolved Analysis of Pulse Envelope and Phase

This study focuses exclusively on the temporal evolution of the electric field, adopting a spatially homogeneous model where $E(x, y, z, t) \equiv E(t)$. Although the physical electric field is strictly real-valued, we employ a complex analytic representation $E(t)$ for mathematical convenience.

This approach: Simplifies analysis by enabling phase-amplitude decomposition ($E(t) = A(t)e^{i\phi(t)}$); Preserves physical meaning since measurable fields correspond to Re$[E(t)]$; Facilitates spectral-domain transformations via Fourier methods.

$$\tilde{E}(t) = \tilde{A}(t) \cdot e^{-iw_0 t} \tag{2}$$

The complex envelope $\tilde{A}(t)$ is conventionally defined such that the physical electric field corresponds to twice the real part of this complex representation, with ω_0 representing the central carrier frequency (typically chosen as the spectral midpoint). This formulation separates the rapidly oscillating carrier (at frequency ω_0) from the slowly varying envelope $A(t)$.

$$\tilde{E}(t) = \left|\tilde{E}(t)\right| \cdot e^{i\varphi_0} \cdot e^{-i\varphi(t)} = \left|\tilde{E}(t)\right| \cdot e^{i\varphi_0} \cdot e^{-i(\emptyset(t) - w_0)} \tag{3}$$

The term $\varphi(t)$ represents the temporal phase of the pulse, whereas φ_0 represents the absolute phase, which defines the alignment between the carrier wave and pulse envelope (see Figure 1). Note that $\emptyset(t)$ excludes the dominant linear term wt associated with the carrier frequency. The absolute phase φ_0 becomes critically important for few-cycle pulses, influencing processes such as high-harmonic generation and carrier-envelope phase effects.

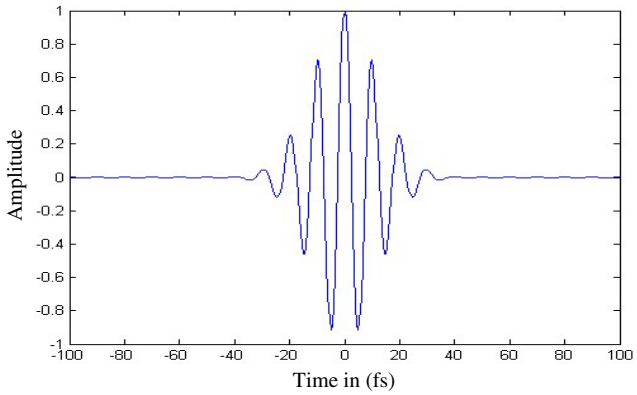

FIGURE 1. The time-dependent electric field $E(t)$ of an ultrashort optical pulse comprising just a few oscillation cycles.

The instantaneous frequency $w(t)$ of a pulse is defined as the time derivative of its temporal phase $\varphi(t)$, given by:

$$w(t) = \frac{d\varphi(t)}{dt} = \frac{d\emptyset(t)}{dt} - w_0 \tag{4}$$

Consequently, any nonlinearity in the temporal phase $\varphi(t)$ produces a time-dependent frequency modulation $\omega(t)$. This phase-to-frequency conversion characterizes chirped pulses, where the instantaneous frequency varies across the pulse envelope (as illustrated in Figure 2).

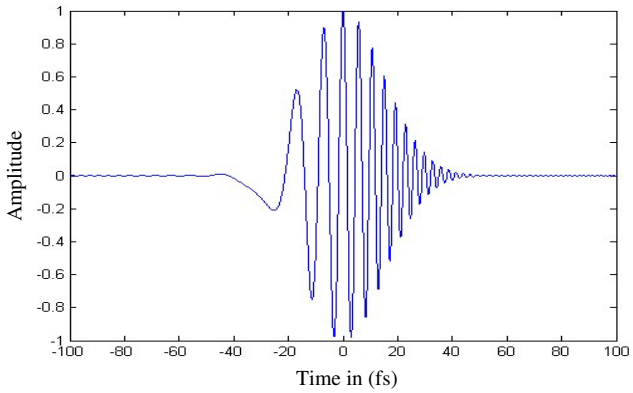

FIGURE 2. Electric field of an ultrashort laser pulse exhibiting strong positive chirp. The temporal variation in frequency is evident, with longer wavelengths (lower frequencies) at the leading edge (left) and shorter wavelengths (higher frequencies) at the trailing edge.

2.1.2. Frequency Domain Description

For most analytical purposes, the frequency-domain representation of the pulse is more convenient than its time-domain counterpart. This spectral form is derived from the temporal electric field using the complex Fourier transform, expressed mathematically as:

$$E(w) = \frac{1}{\sqrt{2\pi}} \int_{-\infty}^{+\infty} E(t) \cdot e^{iwt} \cdot dt \tag{5}$$

Similar to the time domain, $\tilde{E}(w)$ can be expressed as:

$$\tilde{E}(w) = \left|\tilde{E}(w)\right| e^{i\varphi(w)} \tag{6}$$

where $\varphi(w)$ represents the spectral phase. Applying the inverse Fourier transform returns the field to the time domain:

$$\tilde{E}(t) = \frac{1}{\sqrt{2\pi}} \int_{-\infty}^{+\infty} \tilde{E}(t) \cdot e^{iwt} \cdot dw \tag{7}$$

Equation (8) shows that the electric field $\tilde{E}(t)$ can be interpreted as a coherent superposition of monochromatic wave components. The measurable spectrum $S(\omega) \equiv |\tilde{E}(\omega)|^2$ provides the spectral energy distribution but does not contain phase information.

The spectral phase $\emptyset(w)$ can be expanded as a Taylor series around the central frequency ω_0:

$$\emptyset(w) = \emptyset_0 + \sum_{n=1}^{\infty} \frac{1}{n!} a_n (w - w_0)^n \tag{8}$$

with $a_n = \frac{d^n \varphi}{dw^n}\Big|_{w=w_0}$.

Substituting this expansion into Equation (8) reveals that the constant and linear phase terms leave the pulse shape unchanged: the constant term only affects the absolute phase, while the linear term introduces a temporal shift. The higher-order terms, however, cause pulse reshaping by altering the relative timing of spectral components. Any nonlinear phase variation modifies the frequency-dependent timing, leading to pulse reshaping.

3. FEMTOSECOND PULSE PROPAGATION THROUGH TRANSPARENT OPTICAL MEDIA

In practical optical systems, all components introduce temporal broadening of ultrashort pulses due to group-velocity dispersion (GVD) acting over their broad spectra. Dispersion management is therefore essential for maintaining pulse integrity [18]. For Gaussian pulses, the spectral shape remains Gaussian under Fourier transformation, and the spectral representation can be written as:

$$E(w) = E_0 \exp\left(\frac{-(w - w_0)^2}{4 \cdot \Gamma}\right) \tag{9}$$

where Γ determines the spectral width of the Gaussian pulse. Upon propagating through distance x, the pulse acquires a modified spectral profile given by:

$$E(w, z) = E(w) \exp\left[\pm ik(w) z\right] \tag{10}$$

with $k(w) = \frac{n(w) \cdot w}{c}$.

The frequency-dependent propagation factor $k(\omega)$ is now expanded as a Taylor series about the central frequency ω_0. This approximation, valid when the bandwidth satisfies $\Delta\omega \ll \omega_0$, enables semi-analytical solutions for pulse propagation effects. While this condition becomes marginal for few-cycle pulses, substituting the Taylor expansion into Equation (11) yields the following spectral representation:

$$k(w) = k(w_0) + k^{'}(w - w_0) + \frac{1}{2} k^{''}(w - w_0)^2 + \cdots \tag{11}$$

where $k^{'} = \left(\frac{dk(w)}{dw}\right)_{w_0}$ and $k^{''} = \left(\frac{d^2 k(w)}{dw^2}\right)_{w_0}$.

$$E(w, z) = \exp\left[-ik(w_0) z - ik^{'} z (w - w_0) - \left(\frac{1}{4\Gamma} + \frac{i}{2} k^{''}\right)(w - w_0)^2\right] \tag{12}$$

We reconstruct the propagated pulse $E(x, t)$ by applying the inverse Fourier transform to the modified spectrum $\tilde{E}(x, \omega)$ from Equation (13).

$$e(t, z) = \int_{-\infty}^{+\infty} E(w, z) \cdot e^{-iwt} dw \tag{13}$$

so that:

$$e(t, z) = \sqrt{\frac{\Gamma(z)}{\pi}} \cdot \exp\left[iw_0 \left(t - \frac{z}{V_\emptyset(w_0)}\right)\right] \times \exp\left[-\Gamma(z) \left(t - \frac{z}{V_g(w_0)}\right)^2\right] \tag{14}$$

where:

$$V_\emptyset(w_0) = (w/k)_{w_0},$$
$$V_g(w_0) = \left(\frac{dw}{dk}\right)_{w_0}, \tag{15}$$
$$1/\Gamma(z) = \frac{1}{\Gamma} + 2ik^{''} z$$

The first exponential term in Equation (15) indicates that the central frequency component ω_0 accumulates a phase delay of $\frac{z}{V_\emptyset}$ during propagation. Although this phase shift affects the complex field representation, it has no physical consequences since:

1. The absolute phase is not experimentally observable.
2. The phase velocity $V_\emptyset(w_0)$ describes the propagation of: Infinite plane wave components, Monochromatic solutions ($\omega = \omega_0$), and Non-informational wavefronts, which extend infinitely in time and therefore carry no localized physical information.

Equation (15) reveals through its second term that the pulse maintains a Gaussian envelope during propagation. This envelope experiences a temporal delay of z/V_g, where V_g represents the group velocity of the pulse.

Analysis of the second term in Equation (15) reveals that pulse propagation causes envelope distortion characterized by the form factor $\Gamma(z)$, where:

$$\frac{1}{\Gamma(z)} = \frac{1}{\Gamma_0} + 2ik^{''} z \tag{16}$$

where Γ_0 is the initial spectral width parameter, and $k^{''}$ is the second derivative of the propagation constant with respect to

angular frequency. This relation describes how the pulse envelope becomes distorted and temporally broadened during propagation through a dispersive medium.

The form factor $\Gamma(z)$ exhibits frequency dependence through its angular frequency (ω) relationship, expressed as $k^{''}(w)$.

$$k^{''} = \left(d^2k/dw^2\right)_{w_0} = \frac{d}{dw}\left(\frac{1}{V_g}\right)_{w_0} \tag{17}$$

The quantity $\beta_2 \equiv \partial^2 k/\partial\omega^2$, known as Group Velocity Dispersion (GVD), characterizes how the medium's group velocity of a medium varies with frequency across its spectral components. Expressed in fs^2/mm, this parameter determines the temporal broadening of the pulse envelope as it propagates, defining the pulse width $\tau(z)$ at a distance z along the propagation axis.

$$\Delta\tau_z = \Delta\tau_0\sqrt{1 + 4\cdot(\Gamma\cdot k''z)^2} \tag{18}$$

with $k^{''} = \frac{\lambda^3}{2\cdot\pi\cdot c^2}\frac{d^2n}{d\lambda^2}$, $\Gamma = \frac{2\log 2}{\Delta_0^2}$.

3.1. Application in Silica

The index of SiO_2 is represented by the following Equation (19):

$$n^2(w) = 1 + \sum_{i=1}^{m}\frac{B_i w_i^2}{w_i^2 - w^2} \tag{19}$$

with:

$$\begin{aligned} B_1 &= 0.6961663; \quad \lambda 1 = 0.0684043\,\mu\text{m} \\ B_2 &= 0.4079426; \quad \lambda 2 = 0.1162414\,\mu\text{m} \\ B_3 &= 0.8974794; \quad \lambda 3 = 9.896161\,\mu\text{m} \end{aligned}$$

where w_i is the frequency of resonance, and B_i is the amplitude of resonance.

In optical fibers, parameters w_i and B_i are experimentally determined by fitting the measured dispersion data to Equation (19) with $m = 3$. These coefficients vary with the material composition of the fiber core, thereby reflecting how the core refractive index profile influences the fiber's dispersive properties [20–21].

3.2. Comparative Analysis of Dispersion Parameters across Different Media

The coefficient C_D can be defined to quantify the magnitude of frequency shifts in the system:

$$C_D = \frac{z}{D} \tag{20}$$

with $D = \frac{\Delta_0^2}{z\cdot k''}$.

Parameter D, known as the dispersion parameter, indicates how significantly chromatic dispersion affects light propagation, while z measures how far the laser pulse travels through the material [19]:

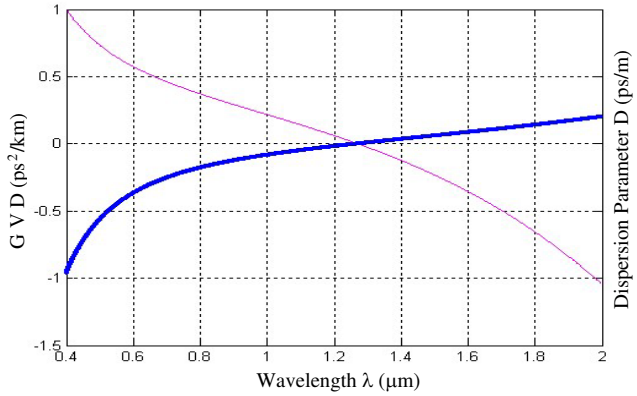

FIGURE 3. The wavelength dependence of group velocity dispersion ($k^{''}$) and the dispersion parameter D (solid line) in SiO_2.

- If $z < D$, second-order dispersion effects ($\beta_2 \approx 0$) are insignificant for these propagation conditions.
- If $z > D$, the inclusion of dispersion terms is essential for complete physical description.

Figure 3 reveals the characteristic zero-dispersion wavelength (ZDW) near 1.27 µm. While $k^{''}$ governs phase-matching in nonlinear processes, D is critical for predicting pulse broadening telecommunication bands.

We analyze the effects of second-order dispersion on pulse propagation. As the pulse advances through the medium, group velocity dispersion (GVD) causes temporal broadening of its envelope. In essence, when an ultrashort optical pulse propagates through a transparent material, it undergoes three primary modifications: a group delay, temporal stretching, and the imposition of a frequency chirp.

3.3. Dispersive Pulse Broadening

Group Velocity Dispersion (GVD) describes the variation in propagation speeds among the different frequency components of a pulse traveling through a dispersive medium. This effect arises from the wavelength dependence of the refractive index of the material. While GVD modifies the temporal profile of the laser pulse, causing it to spread and acquire chirp, it does not alter its spectral amplitude.

A transform-limited pulse, often referred to as a short, unchirped pulse, acquires a positive chirp (up-chirp) after propagating through a normally dispersive medium such as silica glass. In this regime, higher-frequency components (e.g., blue light) travel more slowly than lower-frequency components (e.g., red light). Conversely, in anomalously dispersive media, the pulse develops a negative chirp (down-chirp), where higher frequencies propagate faster than their lower-frequency counterparts.

In our initial analysis, we considered only the second-order term in the Taylor expansion of the phase. It should be noted, however, that Fourier analysis remains applicable solely for pulse durations exceeding approximately 60 fs. Beyond this, we incorporate all higher-order dispersion effects in the medium to ensure a complete description of the physical mechanisms governing ultrashort-pulse propagation.

When higher-order dispersion is taken into account, the pulse not only undergoes temporal broadening but also develops asymmetry, with the off-axis regions of the pulse exhibiting a larger temporal width than the on-axis component [20].

$$\begin{bmatrix} \emptyset^{(2)} \\ \emptyset^{(3)} \\ \emptyset^{(4)} \\ \emptyset^{(5)} \\ \emptyset^{(6)} \end{bmatrix} = (-1)^n 2 \cdot \pi \cdot z \left[\frac{\lambda}{2 \cdot \pi \cdot c}\right]^n$$

$$\begin{bmatrix} 1 & 0 & 0 & 0 & 0 \\ 3 & 1 & 0 & 0 & 0 \\ 12 & 8 & 1 & 0 & 0 \\ 60 & 60 & 15 & 1 & 0 \\ 360 & 480 & 180 & 24 & 1 \end{bmatrix} \quad (21)$$

We can encode the Taylor expansion up to order n in a matrix $[A]$, which compactly captures all the relevant terms A_{ij}.

$$\emptyset(w) = \emptyset(w_0) + (w - w_0)\emptyset^{(1)} + \sum_{i=2}^{p} \frac{1}{i!}(w - w_0)^i \emptyset^{(i)}\Big|_{w=w_0} + \theta(w) \quad (22)$$

$$\emptyset^{(p)} = (-1)^p \cdot 2\pi \cdot z \left[\frac{\lambda}{2 \cdot \pi \cdot c}\right]^p \sum_{j=2}^{p} \lambda^{j-1} A(p-1, j-1) n^{(j)} \quad (23)$$

with $p > 2$.

The propagation effects, including spectral shifts, pulse broadening, and asymmetric distortion in dispersive media (Figure 4 and Figure 5), observed both analytically and experimentally, are accurately replicated in our numerical simulations using the proposed formalism. Furthermore, this method enables the analysis of pulses with arbitrary temporal profiles without adding algorithmic complexity. Importantly, unlike analytical approaches, our numerical framework readily accounts for higher-order dispersion effects [22, 24].

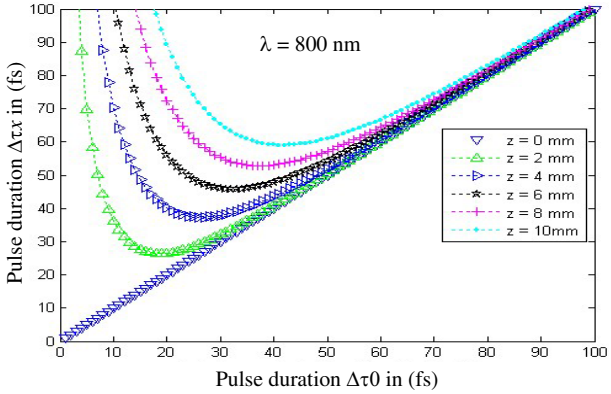

FIGURE 4. Dependence of pulse temporal broadening on propagation distance x for transform-limited pulses.

3.4. Contextual Analysis

The Fourier theorem has traditionally served as the standard approach for modeling electromagnetic signal propagation in dispersive media. For signals exhibiting slowly varying temporal envelopes, the phase is commonly approximated by a Taylor expansion about the pulse's central frequency. However, as pulse durations decrease, the concept of group velocity loses its significance, and envelope distortion becomes dominated by higher-order dispersion terms.

While ultrashort pulses with durations below 10 fs are now achievable, their broad spectral bandwidth renders the phase Taylor expansion less applicable. However, current analysis still relies primarily on numerical evaluation of the Fourier integral, which offers limited physical insight into envelope propagation and often obscures the role of group velocity dispersion in pulse distortion. This limitation underscores the need for an alternative decomposition method that explicitly accounts for the joint time-frequency characteristics of pulse components [25].

Numerous two-dimensional representations exist for analyzing acoustic and electromagnetic signals. Within this framework, we propose a Gabor-transform-based method to decompose signals into an infinite set of elementary wavelets. Each of these components has a uniform temporal duration, significantly longer than that of the original signal, and is centered around a frequency Ω, corresponding to a specific element of the signal's Fourier spectrum [26].

4. ADAPTIVE TIME-FREQUENCY SIGNAL PROCESSING TECHNIQUES

4.1. Mathematical Theory of Wavelets

Wavelet theory emerged in 1983 from Jean Morlet's pioneering work, providing a revolutionary approach to multiscale signal analysis and synthesis. This approach enables the simultaneous examination of signals across multiple scales, effectively combining phenomena operating at vastly different resolutions [23].

Wavelets represent a special class of basis functions characterized as:

- The most elementary and compact oscillations achievable,
- Localized in both time and frequency domains, and
- Capable of performing mathematical "zooming", concentrating analysis on specific signal features at precise locations and scales.

4.2. Time-Frequency Wavelet Analysis for Ultrafast Pulse Characterization

Starting with a signal $e(t)$, in plane $z = 0$, we define wavelet centered at Ω by:

$$\theta(\Omega) = E(w) \cdot \exp\left[-\frac{(w - \Omega)^2}{4\gamma}\right] \quad (24)$$

with $E(w) = \frac{E_0}{2 \cdot \pi}\sqrt{\frac{\pi}{\Gamma}} \exp\left[\frac{(w-w_0)^2}{4 \cdot \Gamma}\right]$.

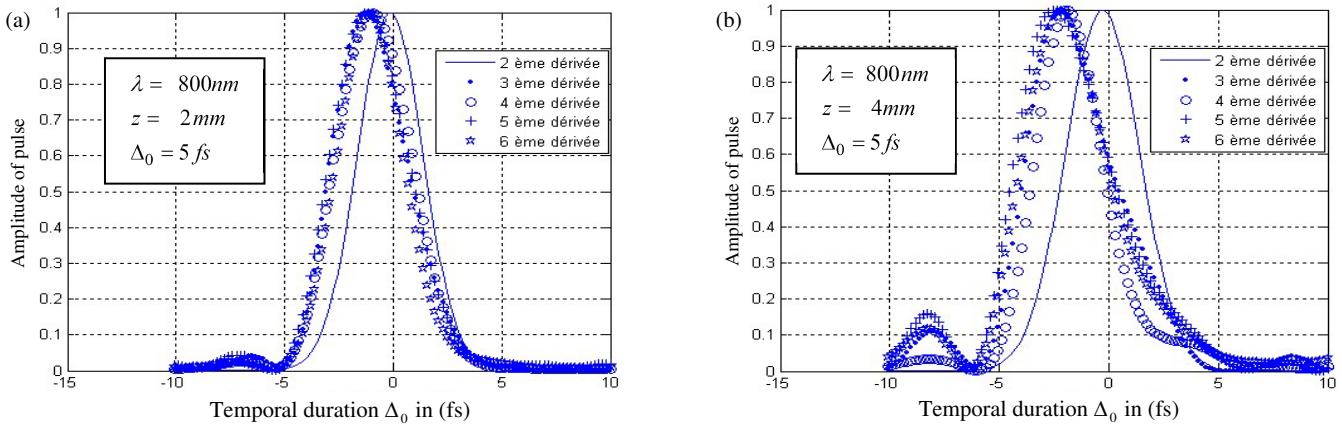

FIGURE 5. (a) The pulse broadens during propagation due to group velocity dispersion (GVD). (b) Due to higher-order dispersions, the pulse shape deviates from a Gaussian profile and becomes asymmetric.

The electric field corresponding to the wavelet component is computed $\theta(\Omega, z=0)$.

$$\theta\left(t, z=0\right) = TF\left\{\theta(\Omega, z=0)\right\} \tag{25}$$

$$\theta\left(t, z=0\right) = E_0\sqrt{\frac{\gamma}{\gamma+\Gamma}}\cdot a\cdot b\cdot c \tag{26}$$

with $a = \exp\left[\frac{-(w_0-\Omega)^2}{4(\gamma+\Gamma)}\right]$, $b = \exp\left[-\frac{\gamma\Gamma}{\gamma+\Gamma}t^2\right]$, $c = \exp\left[j\frac{\gamma w_0+\Gamma\Omega}{\gamma+\Gamma}t\right]$.

The peak amplitude of the wavelet $\theta(t, x=0)$ depends on Ω, the central analysis frequency, for a Gaussian defined by its parameter $\gamma+\Gamma$ [22].

In the time domain, the pulse is also Gaussian-shaped, with its temporal profile determined by the parameter $\frac{\gamma\Gamma}{\gamma+\Gamma}$. The optical signal travels exclusively in the $+x$ direction through a linear, dispersive, and lossless medium occupying the half-space $z>0$. Considering the frequency-dependent refractive index $n(\omega)$, the wavelet component $\theta(\Omega, x)$ takes the following form:

$$\theta\left(\Omega, z\right) = \frac{E_0}{2\cdot\sqrt{\pi\gamma}}E\left(w\right)\cdot\exp\left[-\frac{\left(w-\Omega\right)^2}{4\gamma}\right]\cdot\exp\left[j\emptyset(w)\right] \tag{27}$$

As demonstrated earlier, the wavelet duration τ_{wavelet} is chosen large enough to ensure that the spectral support of the analyzing function remains tightly concentrated around the frequency Ω (see Figure 6).

$$\emptyset(w) = \emptyset\left(\Omega\right) + \left(w-\Omega\right)\left.\frac{d\emptyset}{dw}\right|_{w=\Omega} + \frac{1}{2!}\left(w-\Omega\right)^2\left.\frac{d^2\emptyset}{dw^2}\right|_{w=\Omega} + \cdots + \frac{1}{n!}(w-\Omega)^n\left.\frac{d^n\emptyset}{dw^n}\right|_{w=\Omega} + \theta\left(w\right) \tag{28}$$

Truncating the equation by removing higher-order terms in Equation (28):

$$\emptyset\left(w\right) = \emptyset\left(\Omega\right) + \left(w-\Omega\right)\left.\frac{d\emptyset}{dw}\right|_{w=\Omega}$$

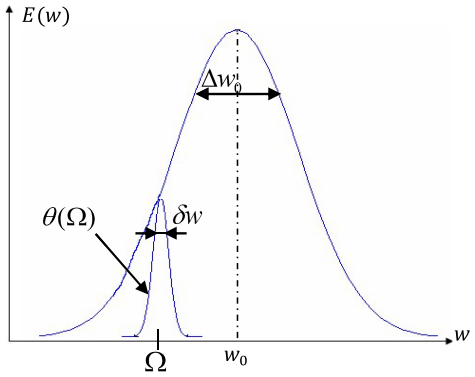

FIGURE 6. The Gaussian envelope is analyzed through a continuous wavelet transform.

$$+\frac{1}{2!}\left(w-\Omega\right)^2\left.\frac{d^2\emptyset}{dw^2}\right|_{w=\Omega} + \cdots + \theta\left(w\right) \tag{29}$$

$$\theta\left(\Omega, z\right) = \frac{E_0}{2\cdot\sqrt{\pi}\gamma}\sqrt{\frac{\pi}{\Gamma}}\exp\left[-\frac{\left(w-w_0\right)^2}{4\Gamma}\right]\cdot a \tag{30}$$

with $a = \exp\left[-\frac{(w-\Omega)^2}{4\gamma}\right]\cdot\exp[j\emptyset^{(0)} + j\left(w-\Omega\right)\emptyset^{(1)} + \frac{1}{2}j\left(w-\Omega\right)^2\cdot\emptyset^{(2)}]$.

Using inverse Fourier transformation, we reconstruct the time-domain electric field for each wavelet component $\theta(\Omega, z)$.

$$\theta\left(t, z\right) = \frac{1}{2\pi}\int_{-\infty}^{+\infty}\theta\left(\Omega, z\right)\cdot\exp\left(jwt\right)dw \tag{31}$$

$$\theta\left(t, z\right) = \frac{1}{2\pi}\frac{E_0}{2\cdot\sqrt{\pi}\gamma}\sqrt{\frac{\pi}{\Gamma}}e^{\left[-\frac{(\Omega-w_0)^2}{4\Gamma}\right]}e^{\left(j\emptyset^{(0)}\right)} \cdot e^{-\left[\frac{1}{4\Gamma}+\frac{1}{4\gamma}-\frac{1}{2}j\emptyset^{(2)}\right]\Omega^2} \times \int_{-\infty}^{+\infty}e^{-\left[\frac{1}{4\Gamma}+\frac{1}{4\gamma}-\frac{1}{2}j\emptyset^{(2)}\right]w^2} \cdot e^{\left[\frac{1}{4\Gamma}+\frac{1}{4\gamma}-\frac{1}{2}j\emptyset^{(2)}\right]2\Omega w} \times e^{\left[-\frac{(\Omega-w_0)^2}{2\Gamma}-j\emptyset^{(1)}\right]}e^{jwt}dW \tag{32}$$

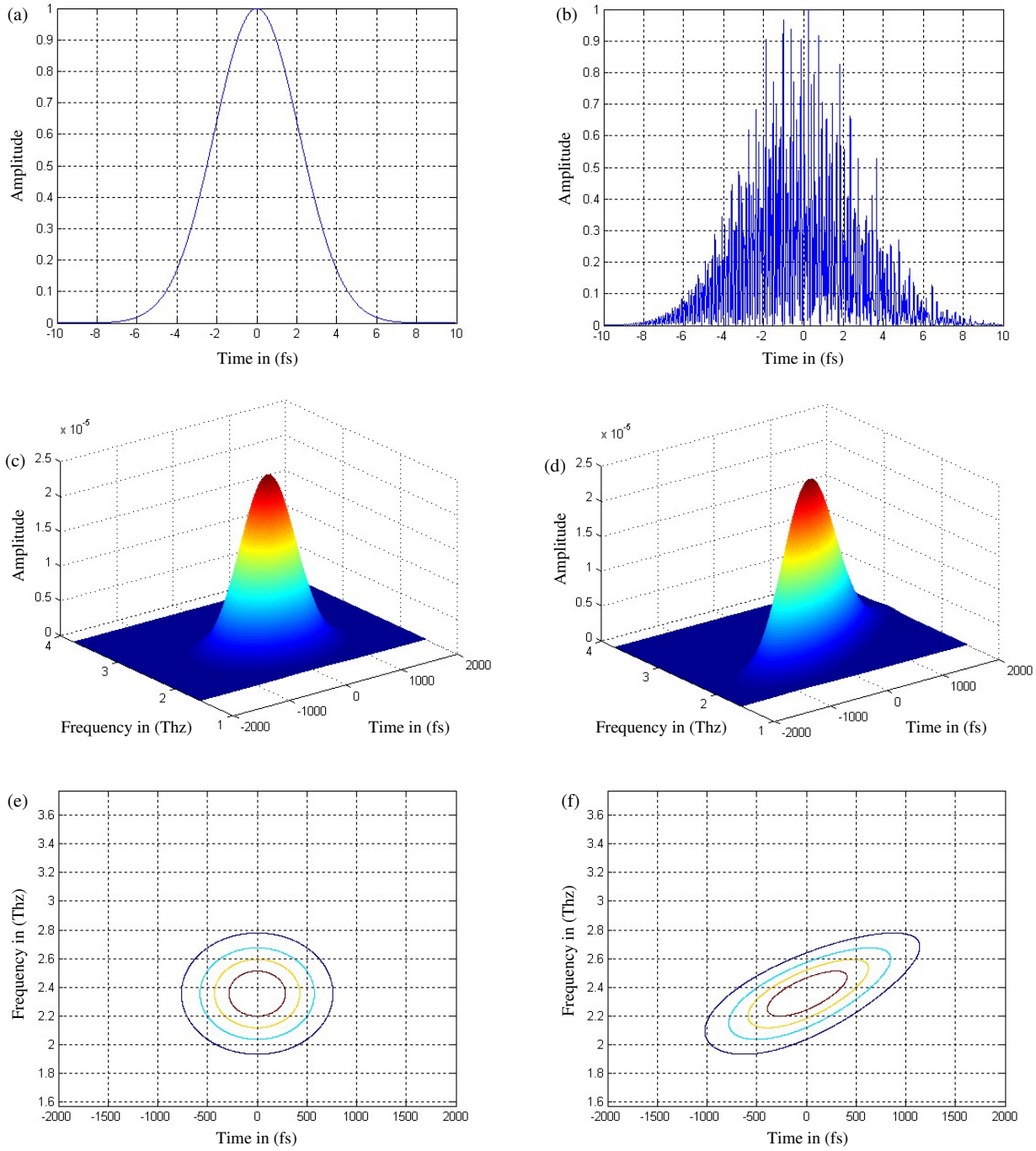

FIGURE 7. (a) Initial pulse, (b) initial wavelet, (c) time-frequency wavelet, (d) the pulse profile after 5 cm of propagation in S_iO_2, (e) the wavelet representation, and (f) time-frequency wavelet after propagation in 5 cm of S_iO_2.

From Equation (33), the amplitude of the incident wavelet at frequency Ω is given by:

$$\theta(t,z) = \frac{E_0}{2\cdot\sqrt{\pi}\gamma}\sqrt{\frac{\Gamma(z)}{\Gamma}}\cdot\exp\left(j\emptyset^{(0)}\right) \exp\left(-\Gamma(z)\times\left[t+\frac{z}{V_g(\Omega)}\right]^2\right) \exp\left(-\frac{(\Omega-w_0)^2}{4\Gamma}\left[1-\frac{\Gamma(z)}{\Gamma}\right]\right) \times\exp\left[j\left(1-\frac{\Gamma(z)}{\Gamma}\right)\Omega+\frac{\Gamma(z)}{\Gamma}w_0\right] \left(t+\frac{z}{V_g(\Omega)}\right) \quad (33)$$

The wavelet is defined by a Gaussian temporal envelope of the form. The decomposition maintains accuracy strictly within the parameter range where Δw is much larger than $\delta w (\Delta w \gg \delta w)$.

The wavelet's group delay, given by $\left[t+\frac{z}{V_g(\Omega)}\right]$ exhibits a Gaussian temporal envelope with characteristic width.

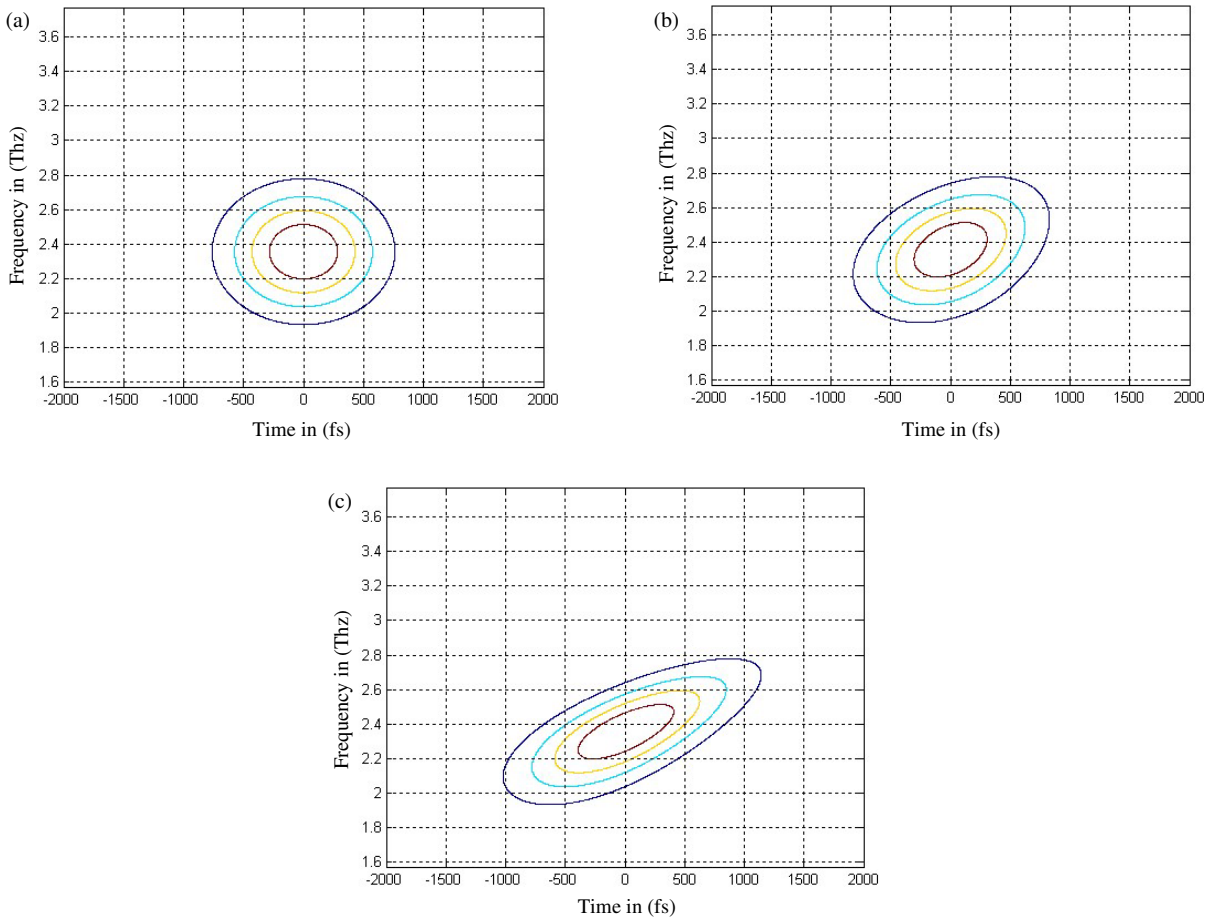

FIGURE 8. (a) Time-frequency wavelet. (b) Time-frequency wavelet after propagation of the 2 cm in the fused silica. (c) Time-frequency wavelet after propagation of the 5 cm in the fused silica.

Measurements confirm the predicted relationship, demonstrating undistorted envelope propagation for each wavelet component [22, 27].

4.3. Computational Modeling Results

Benchmark Parameters for Pulse Propagation Simulations

Initial pulse width: $\Delta\tau_0 = 5\,\text{fs}$
Wavelength: $\lambda = 800\,\text{nm}$
Wavelet width: $\Delta\tau_{\text{wavelet}} = 1000\,\text{fs}$
Distance of the propagation: $z = 5\,\text{cm}$

Our pulse characterization methodology tracks the propagation dynamics through wavelet maxima trajectories in a three-dimensional parameter space (time, frequency, and amplitude).

This section elucidates the operational principles and simulation results of the wavelet-based decomposition technique. Figure 6 presents a conceptual schematic illustrating the fundamental mechanism of the wavelet technique. It depicts how an optical pulse can be decomposed into its constituent wavelets, thereby enabling a detailed time-frequency analysis of its evolution during propagation. Figures 7(a)–(f) display the simulation results of pulse propagation through a 5 cm silica fiber over a duration of 1000 fs. Figure 7(a) shows the initial pulse, while Figures 7(b) and 7(c) illustrate the corresponding wavelet energy and time-frequency representation, respectively. After propagation through the fiber, the output pulse is depicted in Figure 7(d). The post-propagation wavelet energy and time-frequency distributions are shown in Figures 7(e) and 7(f). Notably, the time-frequency profile in Figure 7(f) is consistent with the Heisenberg uncertainty principle, reflecting the trade-off between temporal and spectral resolutions. Figure 8 further investigates the pulse dynamics by comparing the time-frequency distributions obtained for different fiber lengths, thereby highlighting the evolution of dispersion and nonlinear effects as the propagation distance increases.

4.4. Comparison and Validation

Finally, Figure 9 presents a comparative analysis demonstrating that the proposed wavelet-based method outperforms alternative techniques, including the widely used Frequency-Resolved Optical Gating (FROG) method [28]. The results confirm that the wavelet approach provides a more powerful and flexible solution for the characterization and measurement of ultrashort optical pulses.

This work validates a novel simulation for ultrashort pulse characterization based on a wavelet technique by comparing its performance against the established third-order FROG method.

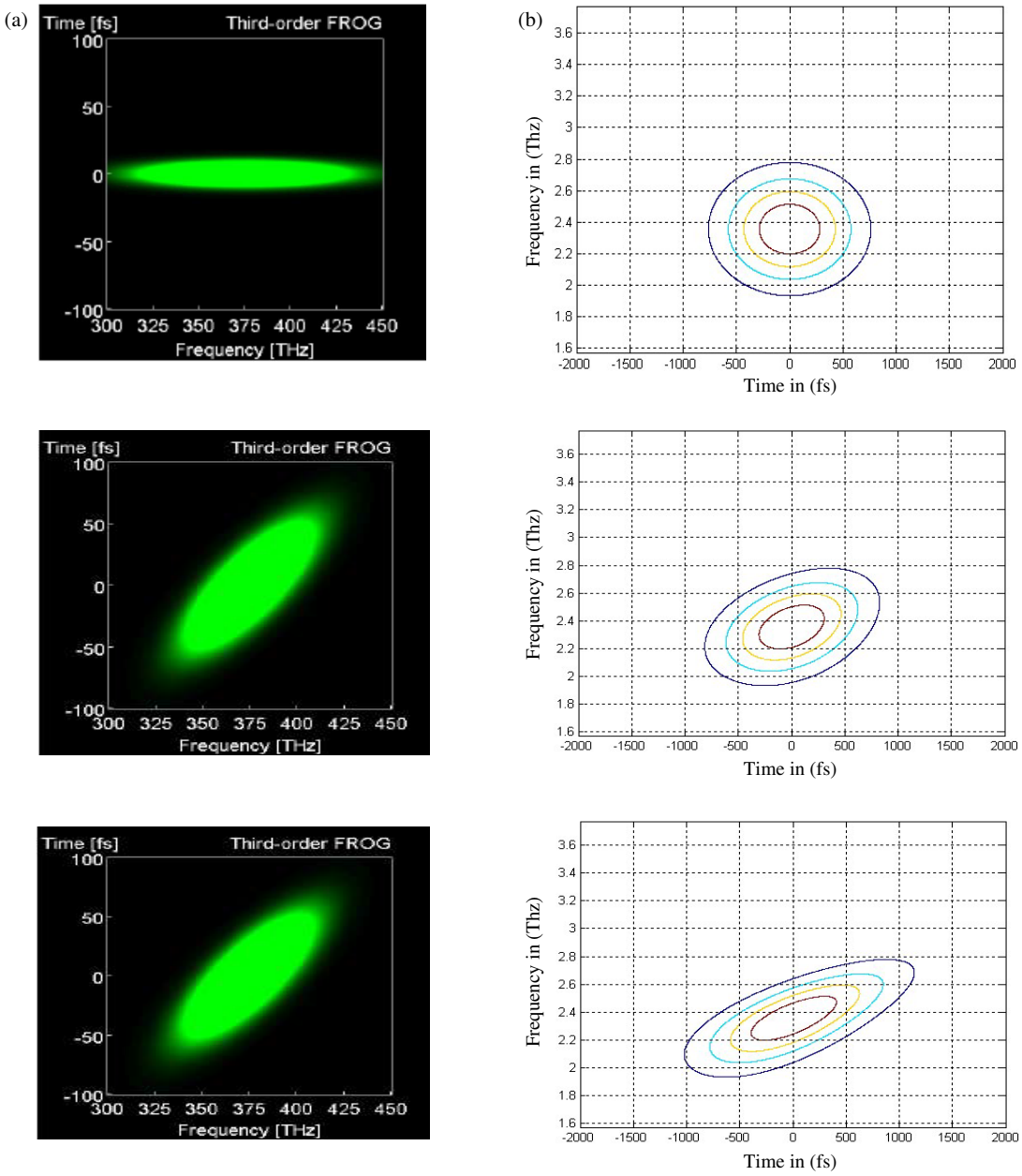

FIGURE 9. Comparison with (a) the third-order FROG technique and (b) our wavelet technique.

The results demonstrate that our wavelet-based approach yields accurate and reliable characterizations. A key distinction between the methods lies in their underlying principles: while the third-order FROG technique relies on an iterative algorithm to retrieve the pulse profile from a spectrogram generated by a nonlinear gating process, our proposed method utilizes a direct transformation framework based on the Fourier and Wavelet transforms, offering a computationally distinct pathway to the solution.

5. CONCLUSION

In this work, we have developed and validated a wavelet-based time-frequency analysis framework for modeling ultrashort pulse propagation in transparent dispersive media. Unlike conventional Fourier-based methods, which provide limited insight into localized time-frequency behavior, the proposed approach enables a joint temporal and spectral analysis of pulse evolution.

The study demonstrates that ultrashort optical pulses can be accurately decomposed into an infinite series of Fourier-transform-limited wavelets, each of which propagates undistorted through a dispersive medium. This decomposition provides a powerful visualization tool for tracking the three-dimensional evolution of the pulse in terms of time, frequency, and amplitude, while offering quantitative assessment of phenomena such as temporal broadening, chirp generation, and spectral shifting.

The results confirm excellent agreement between the wavelet-based simulation and analytical or experimental data,

validating the model's ability to reproduce the main features of ultrashort pulse propagation. Furthermore, the framework's mathematical generality makes it easily extendable to more complex conditions, including absorbing or nonlinear media, where refractive indices vary dynamically with time and intensity.

Although the method provides superior resolution and interpretability compared to purely Fourier-domain approaches, it introduces certain computational and experimental challenges. They include the need for precise phase and amplitude reconstruction, higher computational cost for full time-frequency mapping, and increased experimental complexity in high-resolution implementations.

Despite these challenges, the developed framework constitutes a robust and versatile analytical tool for investigating ultrafast pulse dynamics. Its capacity to separate dispersive effects from intrinsic pulse properties opens new perspectives for applications in ultrafast optics, optical communication, pulse compression, and nonlinear photonics.

REFERENCES

[1] Christov, I. P., "Propagation of femtosecond light pulses," *Optics Communications*, Vol. 53, No. 6, 364–366, 1985.

[2] Ziolkowski, R. W. and J. B. Judkins, "Propagation characteristics of ultrawide-bandwidth pulsed Gaussian beams," *Journal of the Optical Society of America A*, Vol. 9, No. 11, 2021–2030, 1992.

[3] Sheppard, C. J. R. and X. Gan, "Free-space propagation of femtosecond light pulses," *Optics Communications*, Vol. 133, No. 1-6, 1–6, 1997.

[4] Agrawal, G. P., "Spectrum-induced changes in diffraction of pulsed optical beams," *Optics Communications*, Vol. 157, No. 1-6, 52–56, 1998.

[5] Kaplan, A. E., "Diffraction-induced transformation of near-cycle and subcycle pulses," *Journal of the Optical Society of America B*, Vol. 15, No. 3, 951–956, 1998.

[6] Agrawal, G. P., "Far-field diffraction of pulsed optical beams in dispersive media," *Optics Communications*, Vol. 167, No. 1-6, 15–22, 1999.

[7] Porras, M. A., "Propagation of single-cycle pulsed light beams in dispersive media," *Physical Review A*, Vol. 60, No. 6, 5069, 1999.

[8] Ichikawa, H., "Analysis of femtosecond-order optical pulses diffracted by periodic structure," *Journal of the Optical Society of America A*, Vol. 16, No. 2, 299–304, 1999.

[9] Piestun, R. and D. A. B. Miller, "Spatiotemporal control of ultrashort optical pulses by refractive-diffractive-dispersive structured optical elements," *Optics Letters*, Vol. 26, No. 17, 1373–1375, 2001.

[10] Kempe, M., U. Stamm, B. Wilhelmi, and W. Rudolph, "Spatial and temporal transformation of femtosecond laser pulses by lenses and lens systems," *Journal of the Optical Society of America B*, Vol. 9, No. 7, 1158–1165, 1992.

[11] Mattei, G. O. and M. A. Gil, "Spherical aberration in spatial and temporal transforming lenses of femtosecond laser pulses," *Applied Optics*, Vol. 38, No. 6, 1058–1064, 1999.

[12] Fuchs, U., U. D. Zeitner, and A. Tünnermann, "Ultra-short pulse propagation in complex optical systems," *Optics Express*, Vol. 13, No. 10, 3852–3861, 2005.

[13] Sereda, L., A. Ferrari, and M. Bertolotti, "Diffraction of a time Gaussian-shaped pulsed plane wave from a slit," *Pure and Applied Optics: Journal of the European Optical Society Part A*, Vol. 5, No. 4, 349, 1996.

[14] Hwang, H.-E. and G.-H. Yang, "Far-field diffraction characteristics of a time-variant gaussian pulsed beam propagating from a circular aperture," *Optical Engineering*, Vol. 41, No. 11, 2719–2727, 2002.

[15] Liu, Z. and B. Lü, "Spectral shifts and spectral switches in diffraction of ultrashort pulsed beams passing through a circular aperture," *Optik*, Vol. 115, No. 10, 447–454, 2004.

[16] Hwang, H.-E., G.-H. Yang, and P. Han, "Near-field diffraction characteristics of a time-dependent Gaussian-shaped pulsed beam from a circular aperture," *Optical Engineering*, Vol. 42, No. 3, 686–695, 2003.

[17] Wyrowski, F. and J. Turunen, "Wave-optical engineering," in *International Trends in Applied Optics*, A. H. Guenther, Ed., SPIE Press, Bellingham, WA, 2002.

[18] Rullière, C., *Femtosecond Laser Pulses: Principles and Experiments*, Springer, 1998.

[19] Marcuse, D., *Light Transmission Optics*, Ch. 8 and 12, Van Nostrand Reinhold, New York, NY, 1982.

[20] Koch, F., S. V. Chernikov, and J. R. Taylor, "Dispersion measurement in optical fibres over the entire spectral range from 1.1 μm to 1.7 μm," *Optics Communications*, Vol. 175, No. 1-3, 209–213, 2000.

[21] Adams, M. J., *An Introduction to Optical Waveguide Theory*, Chapman and Hall, London, U.K., 1983.

[22] Khelladi, M., "Ultra-short lasers pulses characterizations: Wavelet decomposition," Ph.D. dissertation, Univ. of Tlemcen, Algeria, 2005.

[23] Meyer, Y., S. Jaffort, and O. Rioul, *Wavelet Analysis*, Éditions de la Société Française de Sciences, Paris, France, 1987.

[24] Cai, Y., Z. Chen, X. Zeng, H. Shangguan, X. Lu, Q. Song, Y. Ai, S. Xu, and J. Li, "The development of the temporal measurements for ultrashort laser pulses," *Applied Sciences*, Vol. 10, No. 21, 7401, 2020.

[25] Alonso, B., A. Döpp, and S. W. Jolly, "Space-time characterization of ultrashort laser pulses: A perspective," *APL Photonics*, Vol. 9, No. 7, 070901, 2024.

[26] Jolly, S. W., O. Gobert, and F. Quéré, "Spatio-temporal characterization of ultrashort laser beams: A tutorial," *Journal of Optics*, Vol. 22, No. 10, 103501, 2020.

[27] Gao, W., S. W. Kim, H. Bosse, and K. Minoshima, "Dimensional metrology based on ultrashort pulse laser and optical frequency comb," *CIRP Annals*, Vol. 74, No. 2, 993–1018, 2025.